The Canadian Mineralogist
Vol. 35, pp. 275-290 (1997)

PRIMITIVE K-RICH MAGMAS FROM CLARK VOLCANO, SOUTHERN KERMADEC ARC: A PARADOX IN THE K – DEPTH RELATIONSHIP

JOHN A. GAMBLE[1] AND ROB H.K. CHRISTIE

Department of Geology, Victoria University of Wellington, P.O. Box 600, Wellington, New Zealand

IAN C. WRIGHT

National Institute of Water and Atmospheric Research, P.O. Box 14-901. Kilbirnie, Wellington, New Zealand

RICHARD J. WYSOCZANSKI

Research School of Earth Sciences, Australian National University, GPO Box 4, Canberra, ACT, 2601, Australia

ABSTRACT

Clark volcano is the last significant volcanic edifice in the oceanic segment of the nearly 3000-km-long Tonga – Kermadec – New Zealand volcanic arc system, which becomes continental in the Taupo Volcanic Zone of New Zealand. Clark volcano is a submarine basaltic andesite – dacite edifice with broadly similar petrochemical affinity to the rest of the Kermadec island arc (*i.e.*, lavas are mostly of basalt – basaltic andesite composition, with ~0.2% K_2O at 50% SiO_2, MgO in the range 5 to 7%, $(Ce/Yb)_n$ between <1 and 2), but also present is a suite of unusual K-rich basalts. The latter show ~2% K_2O at 50% SiO_2, ~9% MgO, high levels of Ni (>100 ppm) and Cr (>200 ppm), and $5 < (Ce/Yb)_n < 7$; these basalts are unique within the Kermadec – New Zealand subduction regime. Phenocryst assemblages in the K-rich basalts at Clark are olivine (± chromian spinel) + clinopyroxene, which contrast with the plagioclase + olivine ± clinopyroxene assemblages in "typical" Kermadec Arc basalts. In addition to high levels of K and the light rare-earth elements, the K-rich suite shows high concentrations of Ba (~600 ppm), Rb (40 – 60 ppm) and Cs (~1 ppm). Radiogenic isotopes of Sr, Nd and Pb in the K-rich basalts are enriched relative to other magmas of the *oceanic* Kermadec Arc, including those of the more "typical" Clark basalts, and overlap with those of basalts from the *continental* Taupo Volcanic Zone of New Zealand. We interpret these primitive K-rich lavas as a rare example of near-slab, small-volume melts of a mantle wedge source enriched by sediment and fluid transfer from the descending slab of lithosphere. The nature of this subducting slab is significant, because it comprises crust of the Hikurangi Plateau, an anomalously thick sequence of Cretaceous basalt basement and sedimentary basin fill, which is subducting beneath the present-day *continental* Taupo Volcanic Zone and the *oceanic* southern Kermadec Arc.

Keywords: arc geochemistry, primitive K-rich magmas, sediments, Kermadec Arc, southwestern Pacific.

SOMMAIRE

Le volcan Clark est le dernier édifice volcanique du secteur océanique de l'arc Tonga – Kermadec – Nouvelle-Zélande, presque 3000 km de long, avant qu'il ne devienne continental dans la zone volcanique de Taupo, en Nouvelle-Zélande. Il s'agit d'un volcan sous-marin à andésite basaltique – dacite, dont le spectre pétrochimique ressemble en général à celui des autres volcans de l'arc insulaire de Kermadec. Plus précisément, la plupart des coulées ont une composition dans l'intervalle basalte à andésite basaltique, avec environ 0.2% de K_2O à une teneur en SiO_2 de 50%, entre 5 et 7% de MgO, et un rapport $(Ce/Yb)_n$ allant de <1 à 2. Dans la même structure, il se trouve une suite de basaltes enrichis en K, c'est-à-dire environ 2% K_2O à 50% de SiO_2, contenant environ 9% de MgO, des teneurs élevées en Ni (>100 ppm) et Cr (>200 ppm), avec $(Ce/Yb)_n$ entre 5 et 7. Cette suite étrange semble unique dans le système de subduction Kermadec – Nouvelle-Zélande. Les basaltes riches en K contiennent, comme assemblage de phénocristaux, olivine (± spinelle chromifère) + clinopyroxène, ce qui diffère nettement de l'assemblage plagioclase + olivine ± clinopyroxène dans les basaltes plus typiques de l'arc de Kermadec. En plus d'un enrichissement en K et en terres rares légères, les basaltes riches en K possèdent des teneurs élevées en Ba (environ 600 ppm), Rb (entre 40 et 60 ppm), et Cs (environ 1 ppm). Leurs teneurs en isotopes radiogéniques de Sr, Nd et Pb sont plus élevées que dans les autres venues basaltiques du secteur océanique de l'arc de Kermadec, par exemple, les basaltes normaux du même volcan, et ressemblent davantage à celles des basaltes du secteur continental de l'arc, dans la zone volcanique de Taupo, en Nouvelle-Zélande. Nous interprétons ces laves primitives riches en K comme une manifestation assez rare de magmas issus par fusion partielle restreinte du coin de manteau près de la zone de subduction, dont la source a été enrichie par un apport de sédiment et une contribution par

[1] *E-mail address*: john.gamble@vuw.ac.nz

transfert via une phase fluide issue de la plaque lithosphérique en subduction. La nature de cette plaque revet ici une signification particulière; il s'agit de la croûte anormalement épaisse du plateau de Hikurangi, faite d'un socle de basaltes crétacés et d'un remplissage de bassin sédimentaire, qui est présentement en situation de subduction sous la partie continentale de l'arc, et donc sous la zone volcanique de Taupo, ainsi que sous sa partie océanique, dans le secteur sud de l'arc de Kermadec.

(Traduit par la Rédaction)

Mots-clés: géochimie des roches d'arc, magmas primitifs riches en K, sédiments, arc insulaire de Kermadec, secteur sud-ouest du Pacifique.

INTRODUCTION

For many years, the Tonga – Kermadec subduction system has been recognized as an archetypal example of a primitive oceanic island-arc (Ewart *et al.* 1977, Ewart & Hawkesworth 1987). This region has played a major role in the development of models and ideas on marginal basins and backarc basins (Karig 1970, 1971), and was the focus of Leg 135 of the Ocean Drilling Program in 1990 – 1991 (Hawkins *et al.* 1994). The southern extension of the Tonga – Kermadec Island Arc toward New Zealand is represented by submarine volcanoes, which have only recently been surveyed in detail (Gamble *et al.* 1993b, 1994, Wright 1994, Gamble & Wright 1995). These volcanoes, from the north, include the Silent II and Rumble (II, III and IV) seamounts (Smith & Brothers 1988, Gamble *et al.* 1993b) and three more recently surveyed edifices named Rumble V, Tangaroa and Clark (Wright 1994). Southwest of Clark volcano, a major change in slope of the sea floor delineates the transition from oceanic arc, with volcanoes constructed on oceanic crust, to continental arc, where volcanoes are constructed on continental crust. Whakatane volcano, a basaltic andesite – andesite edifice with local relief of some 1100 meters (Fig. 1), marks the northern limit of the offshore segment of the *continental* Taupo Volcanic Zone (TVZ) (Wright 1992, Gamble *et al.* 1993b). It is also significant that the Hikurangi Plateau (Lewis 1994, Wood & Davy 1994, Mortimer & Parkinson 1996) comprises the upper portion of the lithospheric slab subducting presently beneath the continental (TVZ) *and* the oceanic (southern Kermadec Arc) portions of the plate boundary (Fig. 1) along the Hikurangi Trough. The Hikurangi Plateau has a crustal thickness of 10–15 km (as determined by gravity modeling: Davy & Wood 1994) compared to 5–7 km for normal oceanic crust to the northeast, which is subducting beneath the northern Kermadec Arc. Furthermore, seismic reflection profiling indicates that the Hikurangi Plateau basement has a Mesozoic to Cenozoic sedimentary cover up to several kilometers thick (Wood & Davy 1994). The Hikurangi Trough is partially infilled by sediment.

Clark volcano is a large volcanic structure, constructed on *oceanic* crust and whose local relief is about 1600 m (Wright 1994). During dredge sampling of the volcano, an unusual suite of K-rich (1.5 – 2.25% K_2O at 50% SiO_2) basaltic rocks were recovered, in addition to lavas (basaltic andesite, andesite and dacite) of more "typical" Kermadec Arc (KA) character (~0.3% K_2O at 52.6% SiO_2 in basaltic andesite).

Elsewhere, the presence of K-rich volcanic rocks in island-arc suites has been associated with depth to the Wadati – Benioff Zone (Hatherton & Dickinson 1969, Marsh & Carmichael 1974), length of the mantle melting column (Plank & Langmuir 1988), or enrichment processes in the sub-arc mantle (Edwards *et al.* 1991). In this paper, we present new whole-rock geochemical and mineral data on suites from Clark volcano, and other volcanoes toward the southern extremity of the KA system. We compare these data to results of previous studies from the KA (Ewart & Hawkesworth 1987, Smith & Brothers 1988, Gamble *et al.* 1990, 1993a, b), and develop a model to account for the petrogenesis of the K-rich suite of basaltic rocks.

ANALYTICAL TECHNIQUES

All samples reported in this work were collected by dredging on the submarine volcanic edifices during research cruises in 1988 – 1992; see Wright (1994) for details. Samples used for petrological study were selected on the basis of freshness, as determined by study of broken dredge-haul samples. Many contain fresh glass, which was carefully prised from pillow rind surfaces. Prior to crushing, all samples were thoroughly washed with distilled water in an ultrasonic bath and oven-dried at 110°C. Samples were then reduced to cm-sized chips, rewashed and dried, and crushed to a powder in a tungsten carbide ring mill. This powder was used for standard X-ray fluorescence (XRF) techniques in the Analytical Facility of Victoria University and Instrumental Neutron Activation Analysis (INAA); all isotope analyses were undertaken on selected rock-chips.

Mineral analyses were made by electron microprobe in the Analytical Facility of VUW, using a JEOL 733 Superprobe and full ZAF-correction procedures. Concentrations of major element (oxides) and trace elements (Sc, V, Cr, Ni, Cu, Zn, Ga, Rb, Sr, Y, Zr, Nb, Ba, Pb) were determined by standard XRF methods in the Analytical Facility, VUW (Palmer 1990). In most cases, our precision for the trace elements is better than 5% (relative). Increased counting times were employed in the case of Nb, which extended the theoretical limit of detection to <1 ppm. Concentrations of the rare-earth elements (*REE*), Cs, Hf, Th and U were determined by INAA in the School of Geosciences, New Mexico Institute of Mining and Technology. Sr, Nd and Pb isotopes were measured on a Finnegan MAT 261 multicollector mass spectrometer in the Research School of Earth Sciences, Australian National University. Selected rock-chips for isotopic analyses were first leached with warm HCl, then rinsed in ultrapure water, prior to dissolution. During the period in which analyses were determined, measurements of standards were as follows: La Jolla, $^{143}Nd/^{144}Nd = 0.511878 \pm 13$ ($n = 31$); NBS–987, $^{87}Sr/^{86}Sr = 0.710215 \pm 10$ ($n = 42$); SRM–981, $^{206}Pb/^{204}Pb = 16.937$, $^{207}Pb/^{204}Pb = 15.492$, $^{208}Pb/^{204}Pb = 36.708$ ($n = 109$) (Woodhead *et al.* 1995).

Whole-Rock and Mineral Compositions

Most mafic rocks from the KA consist of high-Al basalt and basaltic andesite, with more than 16.5% Al_2O_3 (Crawford *et al.* 1987, Gamble *et al.* 1990). In these "typical" rocks, phenocryst assemblages are dominated by plagioclase, with olivine ± clinopyroxene; orthopyroxene is present in samples of basaltic andesite (Table 1, Fig. 2A). In the K-rich suite of basalts from Clark (samples C1, C2 and C3), olivine and clinopyroxene comprise the major phenocryst phases, and plagioclase is virtually confined to the groundmass (Table 1, Fig. 2B). A few corroded crystals of plagioclase occur in C1 (Table 1), but are almost certainly xenocrystic. The compositional range of plagioclase, pyroxenes and olivine is shown in Figures 3 and 4.

The groundmass plagioclase in the K-rich basalts averages An_{78} (Fig. 3). In the basaltic andesite – dacite suite, plagioclase is the dominant phenocryst phase (Table 1). Phenocrysts are strongly zoned, and commonly

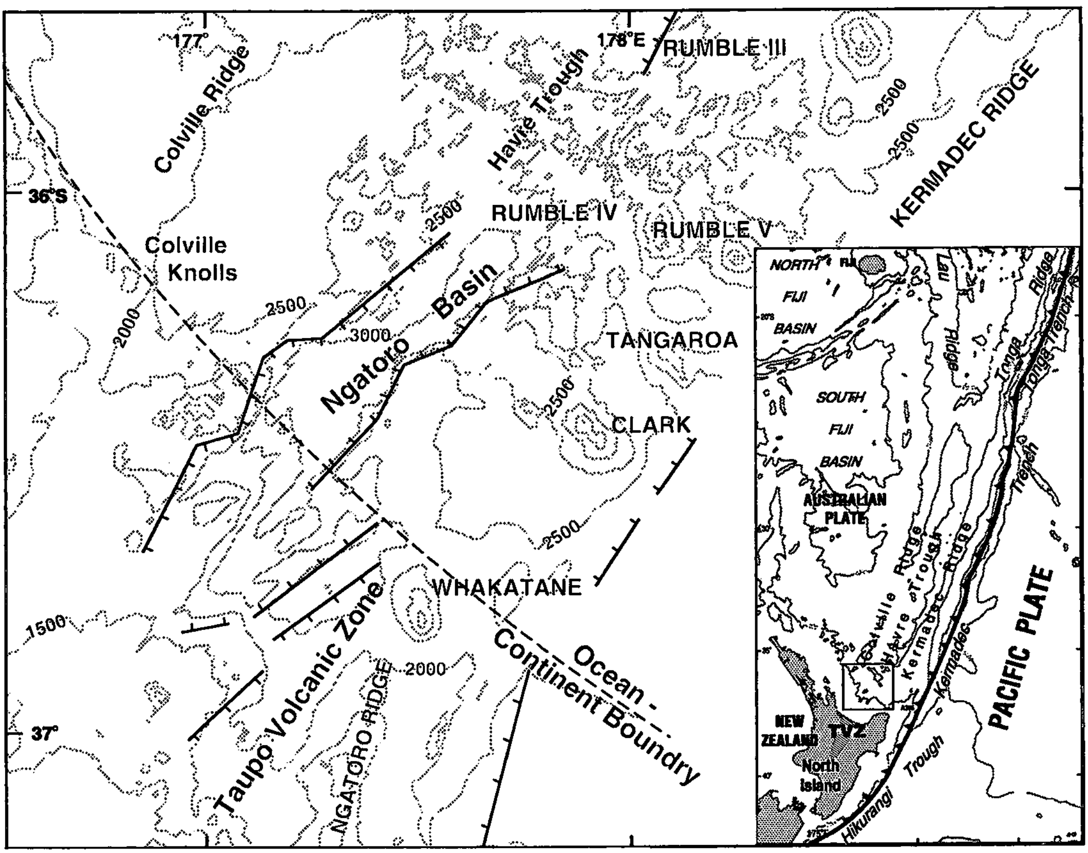

FIG. 1. Location map, adapted from Wright (1994) and Gamble & Wright (1995), showing the submarine volcanoes of the southern Kermadec Arc: Rumble III, IV, V, Tangaroa and Clark. Note how these presently active arc volcanoes lie to the west of the now inactive Kermadec Ridge. The Havre Trough and Ngatoro Basin mark the backarc basin west of the active arc. Whakatane Volcano is the northernmost structure of the offshore segment of the continental Taupo Volcanic Zone, and Colville Knolls consist of Mesozoic greywacke comprising the basement continental crust of New Zealand (Gamble *et al.* 1993). The inset diagram shows major structural elements of the Tonga – Kermadec – New Zealand subduction system; see Wright *et al.* (1996) for details.

TABLE 1. SUMMARY OF MODAL AND COMPOSITIONAL DATA FOR REPRESENTATIVE SAMPLES FROM CLARK VOLCANO

	K-rich Basalt			Basaltic andesite				Dacite
ROCK	C1	C2	C3	C4	C5	C6	C7	C8
Wt% SiO_2 Whole Rock	50.15	50.30	50.45	52.63	55.04	55.05	56.14	63.22
PHENOCRYSTS								
Vol.%	14%	35%	30%	37%	38%	50%	27%	8%
Rel.% of minerals:-								
Plagioclase	<0.5*			50	70	50	73	67
Olivine	64	12	14	3	1	<0.5	1	
Augite	36	88	86	40	20	33	16	20
Orthopyroxene				4	8	15	8	2
Magnetite				3	1	2	2	11
Spinel	trace							
GROUNDMASS								
Vol. %	86%	65%	70%	63%	62%	50%	73%	92%
Minerals present:-								
Plagioclase	Y	Y	Y	Y	Y	(y)	Y	Y
Olivine	Y	Y						
Augite	Y	Y	Y		Y	Y		Y
Subcalcic augite				Y		Y		Y
Pigeonite				Y			Y	Y
Orthopyroxene				Y	Y		Y	Y
Magnetite	(y)	Y	Y	Y	Y	Y	Y	Y
Glass	Y	Y	(y)	(y)	Y	Y	Y	Y
Wt% SiO_2 of glass in:-								
Rock groundmass	60	60-63	62	63	69-70	64	70	devitrfd
Rind groundmass	48-51	51-57	51-55					
Olivine melt inclusions	50-52	52-53	51-58	59				

Note the abundance of phenocrystic plagioclase in the "typical" suite of rocks from the Kermadec Arc (C/4 = 8) and the lack of plagioclase phenocrysts in the K-rich suite. The top row gives the measured (XRF) contents of SiO_2 in the whole rocks. The bottom row shows the range of SiO_2 in the groundmass, glassy pillow rind, and melt inclusions in olivine, as measured with an electron microprobe. The dacite sample (C/8) is entirely devitrified. * Xenocrysts.

show oscillatory zoning and reverse zoning, with compositions extending from An_{92} to An_{53}. Individual samples (Fig. 3) show groundmass compositions that are generally more Na-rich than the phenocrysts, and similar to the extreme outer rim of phenocrysts. The most Ca-rich plagioclase phenocrysts occur in the rocks with lowest SiO_2 content (Table 1, Fig. 3).

Pyroxene compositions are plotted in Figure 4; representative compositions are shown in Table 2. Phenocryst compositions in the K-rich suite (samples C/1, C/2, C/3) are Mg-rich, and straddle the boundary between diopside and augite (Morimoto *et al.* 1988). The core of such pyroxene phenocrysts contains up to ~0.8% Cr_2O_3 and is commonly more Ti-rich than the pyroxene from "typical" KA rocks (Table 2). Groundmass pyroxenes are more Fe-rich and similar to outer-rim compositions of the phenocrysts. In the more "typical" samples from the KA (C/4 to C/8), Ca-rich pyroxene coexists with a Ca-poor pyroxene. Compositions show limited Fe-enrichment and a trend toward a lower Ca content in the groundmass pyroxenes. Overgrowths of pigeonitic compositions on cores of Ca-rich pyroxene (*e.g.*, C/5 and C/7) are indicative of a reaction relationship, possibly associated with mixing events.

Olivine occurs as a phenocryst phase in all samples of basalt and basaltic andesite (samples C1 – C7). In the basalt samples (K-rich suite), the phenocrysts are euhedral, <1 mm across, commonly lantern-shaped, enclose melt inclusions, (Fig. 2), and have a compositional range $Fo_{89} – Fo_{80}$. In two of the basalt samples (C/1 and C/2), olivine also occurs as a groundmass phase, with a composition range $Fo_{81} – Fo_{63}$. In samples of basaltic andesite (C/4 – C/7), the olivine phenocrysts are larger in size (up to 2.5 mm across), but more sparse. They are strongly resorbed and corroded, and lack the euhedral shape characteristic of olivine in the K-rich rocks (Fig. 2). They range in composition from Fo_{90} to Fo_{65}, and some have an outer corona of clinopyroxene or orthopyroxene with an Mg# from 73 to 56, suggestive of reaction relations between crystal and enclosing melt. Inclusions of chromian spinel occur in the olivine phenocrysts of C/1. Finely crystalline magnetite is present in the groundmass of the basalts, gradually increasing to phenocryst status in all the other lavas.

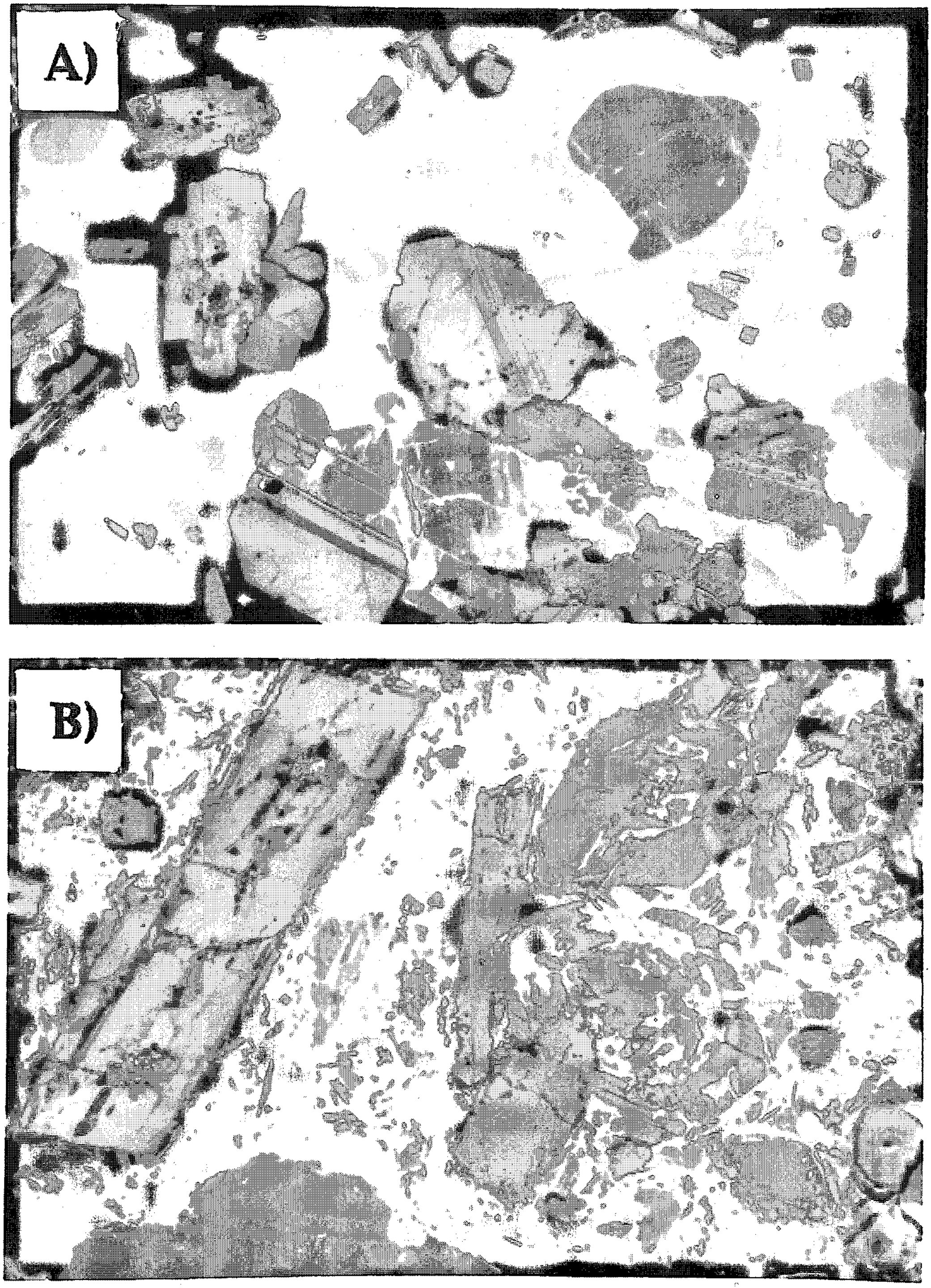

FIG. 2. A. A sample of "typical" Kermadec Arc, Clark Volcano, basaltic andesite (C/4). Note the corroded olivine phenocryst and the phenocryst plagioclase. B. A sample of K-rich basalt (C/3). Note the olivine and clinopyroxene phenocrysts (no plagioclase). Width of field of view 2.5 mm. Both photomicrographs are taken with crossed polars.

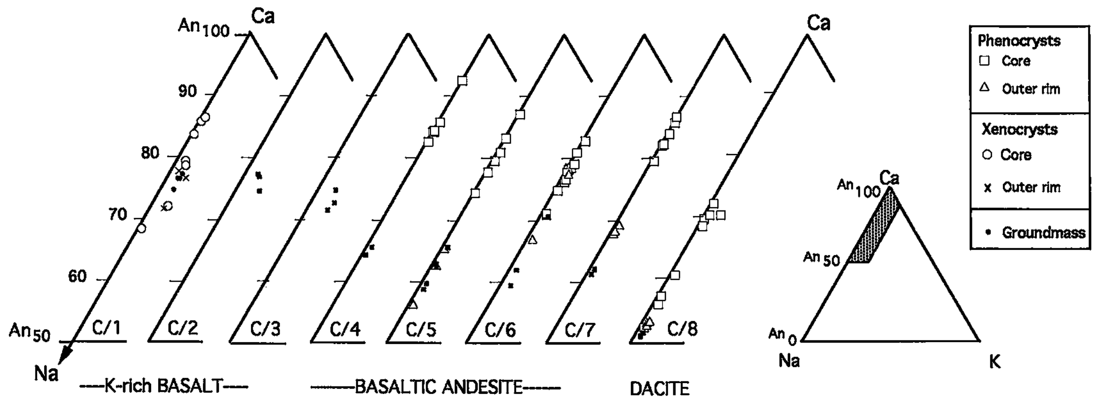

FIG. 3. Compositions of plagioclase in lavas from Clark Volcano in terms of Na – Ca – K (atomic %). Note the rarity of phenocrystic plagioclase in the K-rich basalts (C/1 – C/3).

GEOCHEMISTRY

Representative results of whole-rock analyses are contained in Table 3. The Total Alkali *versus* Silica (TAS, Le Bas *et al.* 1986) and K_2O *versus* SiO_2 diagrams (Figs. 5A, B) highlight the distinctive compositions of the K-rich basalts (C/1, 2 and 3) relative to other rock suites from southern KA volcanoes. In terms of the K_2O – SiO_2 diagram, the K-rich basaltic lavas of Clark volcano are members of the absarokite (C/2 and C/3) and calc-alkaline rock series (C/1). Note that the distinction is marked in Figure 5B, but less so in Figure 5A, which reflects the lower Na content of the Clark magmas as a whole. Chemical differences are also apparent in the rare-earth-element data (Fig. 6A), which show a distinctive light-*REE*-enriched pattern for the K-rich rocks [$(Ce/Yb)_n \approx 6$] relative to the "typical" southern KA rocks from Clark and other adjacent volcanoes. "Typical" KA basalts have flat to slightly *LREE*-enriched patterns [$(Ce/Yb)_n$ <1 to <2]. Moreover, the K-rich rocks display a slightly negative Eu-anomaly, despite the absence of plagioclase from the assemblage of phenocrysts. Multi-element normalized plots (Fig. 6B) illustrate the marked enrichments in elements such as K, Cs, Ba, Rb, Th, the *LREE*, P, Zr and Hf in the K-rich suite relative to typical compositions from the southern Kermadec Arc. These elements are enriched by factors of between 2× and 5× relative to the "typical" KA lavas. In addition, the K-rich basalts show higher Mg-numbers, Ni and Cr contents, and contain chromian-spinel-bearing olivine (~Fo_{90}), all of which are indicative of a primitive character.

The covariation of Sr and Nd isotopes for Clark volcano is shown in Figure 7, along with other comparative data from the region (Gamble *et al.* 1993a, 1994, 1996). Of particular significance are the distinctively radiogenic compositions of the two K-rich samples (C/1 and C/2) relative to the "typical" Clark samples, which plot with other basalts from the southern Kermadec Arc. This distinction also is reflected in the Pb-isotope plots (Fig. 8), which show the K-rich samples within a range defined by the TVZ data, at more radiogenic compositions than the other Clark rocks, which are similar to the southern KA basalts (*cf.* Gamble *et al.* 1993a, 1994, 1996).

DISCUSSION

The relationship between K-content and source depth for subduction-zone magmas has played an important role in the development of petrogenetic models for magmatism at convergent plate-margins (Kuno 1966, Hatherton & Dickinson 1969). The Tonga – Kermadec (oceanic) Island Arc has long been recognized as an example of a primitive arc-system in which magma sources are highly depleted in incompatible elements, arguably due to previous extraction of melt (Ewart *et al.* 1977, Ewart & Hawkesworth 1987, Woodhead *et al.* 1993, Pearce & Parkinson 1993). Extending this model southward to the New Zealand region, Gamble *et al.* (1993a, 1994) identified signs of source heterogeneity, both parallel and normal to the plate boundary, together with an overall increase in source fertility. This was related to the age of the subduction system, with a general younging southward, with present-day volcanism in TVZ "unzipping" the lithosphere of New Zealand (Wright *et al.* 1996). The recovery of K-rich basaltic lavas from Clark volcano, at the presently active volcanic front of the southern KA, was therefore unexpected and unusual, in that primitive K-rich lavas are found associated in space and time with more "typical" KA lavas. Hence the paradox referred to in the title: How can one

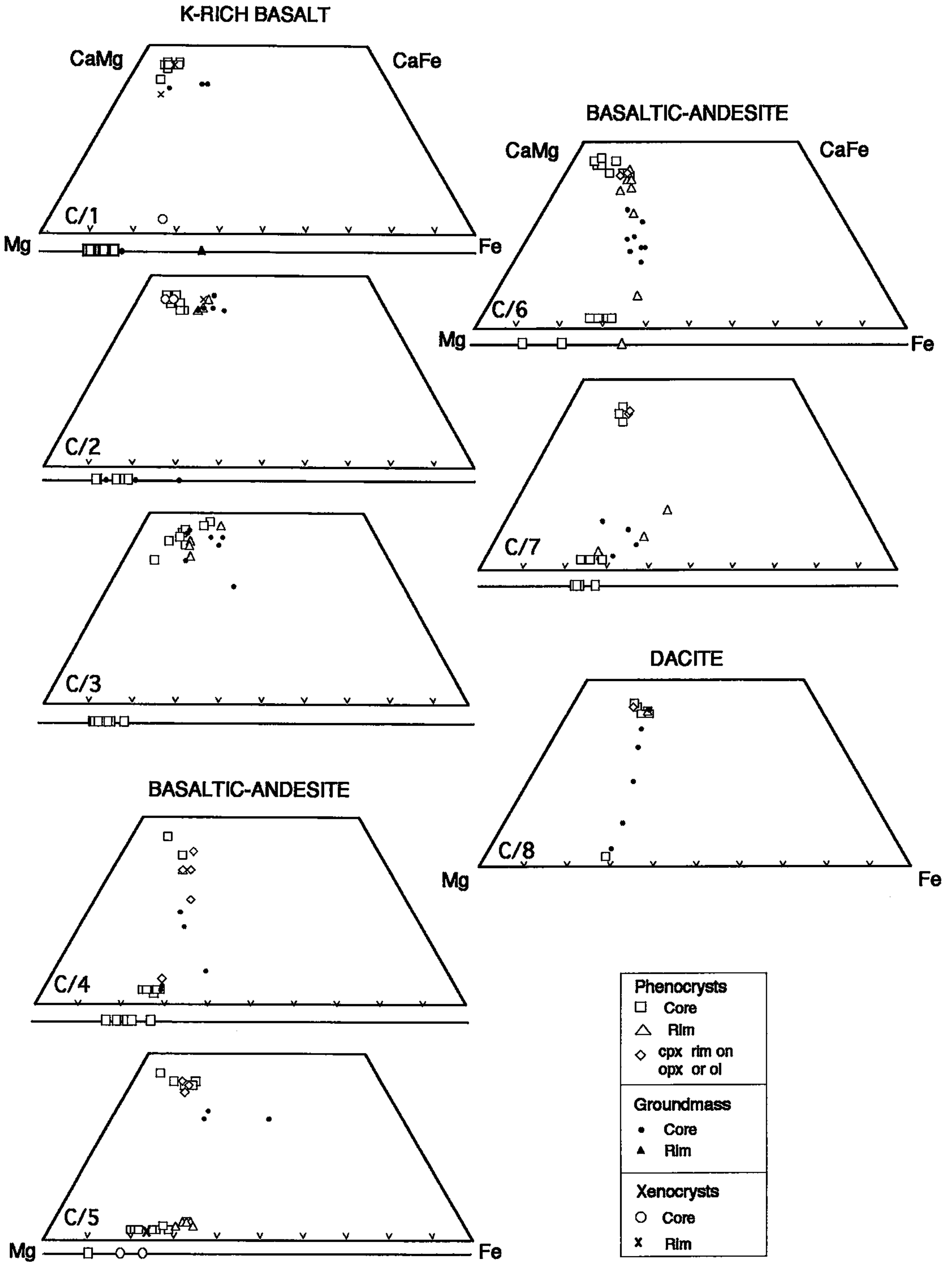

FIG. 4. Compositions of pyroxene and olivine in lavas from Clark Volcano. Note the relatively restricted range of compositions in the K-rich basalts (C/1, 2 and 3) and the more variable compositions in the basaltic andesite – dacite lineage (C/4 – 8).

TABLE 2. REPRESENTATIVE COMPOSITIONS OF PYROXENES FROM K-RICH BASALTS AND BASALTIC ANDESITES FROM CLARK VOLCANO

	K-rich basalts						Basaltic andesite						
Sample:	C/1	C/2	C/2	C/3	C/3	C/3	C/5	C/5	C/5	C/5	C/5	C/5	C/5
	cpx	cpx	cpx	cpx	cpx	cpx	cpx	cpx	cpx	opx	opx	opx	cpx
	Core	Core	Rim	Core	MidZ	Rim	Core	MidZ	Rim	Core	Rim	Orim	Crim
SiO_2	52.12	52.39	48.28	52.37	46.73	50.70	52.36	50.26	50.61	52.85	54.42	52.19	50.20
TiO_2	0.44	0.29	0.89	0.34	1.25	0.59	0.25	0.49	0.32	0.28	0.23	0.29	0.47
Al_2O_3	3.29	2.85	6.56	3.05	8.10	4.62	1.75	2.87	3.27	1.38	1.07	1.34	4.15
FeO	4.11	4.35	9.32	4.69	9.01	7.93	3.34	7.01	5.67	15.95	13.96	18.21	6.90
MnO	0.11	0.15	0.20	0.10	0.19	0.17	0.20	0.37	0.25	0.46	0.47	0.54	0.05
MgO	17.13	17.57	14.35	17.24	12.06	14.99	18.06	15.98	16.67	25.90	28.15	24.09	16.08
CaO	22.66	21.97	19.94	21.17	21.75	20.64	22.65	20.24	21.08	1.74	1.67	1.93	20.52
Na2O	0.21	0.19	0.33	0.18	0.27	0.27	0.33	0.42	0.34	0.09	0.07	0.53	0.22
K2O	0.00	0.11	0.02	0.11	0.17	0.06	0.02	0.07	0.04	0.01	0.01	0.01	0.00
Cr_2O_3	0.74	0.81	0.14	0.63	0.12	0.07	0.63	0.44	0.60	0.28	0.10	0.10	0.11
NiO	0.09	0.04	0.07	0.06	0.07	0.04	0.34	0.10	0.10	0.09	0.07	0.11	0.13
Total	100.90	100.72	100.10	99.94	99.72	100.08	99.93	98.25	98.95	99.03	100.22	99.34	98.83

MidZ indicates a part of a crystal between core and rim. Orim is the extreme outer rim of a phenocryst. Crim stands for the outer rim of clinopyroxene on a phenocryst of orthopyroxene. Electron-microprobe data; the proportion of the major elements is expressed as oxides, in weight %.

reconcile K-rich basaltic lavas adjacent to the arc front of an archetypal primitive and depleted oceanic island-arc? The answer, we believe, is tied in to the unique tectonic setting of the southern Kermadec Arc, where a thick slice of Mesozoic lithosphere (the Hikurangi Plateau) comprises the slab presently subducting beneath continental New Zealand and the oceanic southern Kermadec Arc.

Fate of subducted sediment and fluids along the Hikurangi Margin

Pb isotope ratios are one of the accepted criteria with which to assess sediment involvement in subduction-zone magmas (Armstrong 1971, Hawkesworth *et al.* 1993, Plank & Langmuir 1993). Trace elements such as Cs, Rb, K, Ba and Pb also are typically enriched (by orders of magnitude) in sedimentary source-rocks relative to the putative depleted mantle-wedge source. In combination, these trace elements and isotope ratios are potent means of studying processes of sediment recycling through subduction zones (McCulloch & Gamble 1991, Hawkesworth *et al.* 1993, Plank & Langmuir 1993).

Sediments dredged (unconsolidated) and cored (consolidated) from the Hikurangi Trough and Kermadec Trench have recently been studied in detail (Carter *et al.* 1996, Gamble *et al.* 1996) and a multi-element plot representative of one of these samples is included in Figure 6B. All sediments are strongly enriched in the large-ion lithophile elements (*LILE*), the *LREE*, Pb and Sr, and depleted in Nb, P and Ti relative to the reference backarc basalt from the Havre Trough (Fig. 6B). All samples of sediment also have a negative Eu-anomaly (Gamble *et al.* 1996). These authors described the composition of the sedimentary material in terms of mixing between a continental crust component (New Zealand Mesozoic Torlesse terrane basement), an arc-derived component, and a biogenic component (carbonate ooze). The Torlesse component contributed high U, Th, Pb, *LREE* and radiogenic Sr and Pb isotopes, and is diluted northward by detritus shed from the arc and by carbonate-dominated ooze. Following many other investigators (*e.g.*, Ben Othman *et al.* 1989), it is clear that high abundances of Pb, U, Th, Cs, *LREE* and the relevant Pb isotopes in the sediments would swamp the depleted mantle-wedge, such that input of even traces of sediment into the mantle source would significantly alter the Pb isotope ratios of magmas derived by partial melting. Bulk-mixing calculations (Gamble *et al.* 1996) showed that the addition of as little as 5% sediment into depleted mantle could produce model Pb–Sr–Nd isotopic arrays spanning the entire range of KA – TVZ basalts [*cf.* Vroon *et al.* (1993, 1995) for Indonesia].

However, a number of investigators (*e.g.*, Ellam & Hawkesworth 1988, Hawkesworth *et al.* 1991, 1993, Pearce & Peate 1995) have alluded to a disparity between isotopes and trace elements in terms of mass balance. This decoupling has been attributed to the coexistence of sediment and a (hydrous) fluid component, with a resultant redistribution of trace elements, in particular the alkali metals and the alkaline earths. As a result, ratios of *LILE*/*HFSE* (*e.g.*, Ba/La) have been used with some degree of success to discriminate between fluid and sediment input, with fluid involvement showing

TABLE 3. WHOLE-ROCK COMPOSITION OF REPRESENTATIVE K-RICH AND "TYPICAL" KERMADEC ARC SAMPLES FROM CLARK VOLCANO

	K-RICH BASALTS			BASALTIC ANDESITES				DACITE
Sample	C/1	C/2	C/3	C/4	C/5	C/6	C/7	C/8
SiO_2 wt%	50.15	50.30	50.45	52.63	55.04	55.05	56.14	63.22
TiO_2	0.61	0.62	0.64	0.66	0.72	0.66	0.91	0.65
Al_2O_3	14.11	13.41	13.50	16.25	17.86	16.29	17.43	15.66
Fe_2O_3	1.19	1.22	1.19	1.34	1.07	1.12	1.23	0.67
FeO	7.90	8.15	7.97	8.95	7.15	7.47	8.23	4.46
MnO	0.16	0.17	0.17	0.20	0.15	0.16	0.17	0.16
MgO	9.35	9.00	8.73	6.34	4.51	5.65	3.71	1.83
CaO	11.75	12.75	12.76	11.13	9.73	10.30	8.74	5.07
Na_2O	1.96	1.67	1.69	2.23	2.76	2.62	3.00	3.84
K_2O	1.55	2.18	2.24	0.35	0.60	0.60	0.60	1.60
P_2O_5	0.21	0.27	0.28	0.06	0.08	0.08	0.09	0.21
L.O.I.	0.99	0.48	0.48	0.06	0.47	0.08	-0.06	2.86
Total	99.93	100.22	100.10	100.20	100.14	100.08	100.19	100.23
Mg#	68.3	66.3	66.1	55.8	52.9	57.4	44.6	42.6
Sc ppm	38	37	37	37	29	33	31	17
V	272	283	287	284	253	240	296	57
Cr	416	259	263	74	42	74	12	11
Ni	105	71	73	27	16	21	10	5
Cu	90	119	133	85	111	130	118	11
Zn	67	68	69	76	66	65	81	80
Ga	13	13	13	16	17	15	15	14
Rb	40	53	56	7	11	11	11	20
Sr	340	404	409	194	242	263	227	289
Y	24	27	26	19	21	19	24	34
Zr	83	91	92	45	54	52	57	108
Nb	1	1	1	-	2	2	1	2
Cs	0.77	1.08		0.31	0.44	0.47		0.48
Ba	593	638	635	187	333	312	361	626
La	12.68	16.33		2.50	4.26	3.99		10.79
Ce	26.5	35.7		6.8	10.8	9.1		25.0
Sm	4.40	5.57		1.79	2.22	2.11		4.37
Eu	1.28	1.58		0.67	0.78	0.72		1.30
Tb	0.65	0.74		0.42	0.50	0.47		0.86
Yb	1.81	1.70		1.96	2.10	2.13		3.47
Lu	0.248	0.239		0.276	0.296	0.278		0.527
Hf	1.94	2.30		1.22	1.48	1.41		3.09
Ta	0.083	0.020		0.029	0.065	0.024		0.113
Pb	5	4	3	7	3	4	4	4
Th	1.43	1.64		0.27	0.68	0.61		2.13
U	0.7	0.5						0.5
$^{87}Sr/^{86}Sr$	0.705194	0.705479		0.704138	0.704321			0.704386
st. error	0.000015	0.000009		0.000005	0.000013			0.000011
$^{143}Nd/^{144}Nd$	0.512817	0.512834		0.513091	0.513009			0.512984
st. error	0.000004	0.000012		0.000005	0.000006			0.000008
ϵ Nd	+3.49	+3.82		+8.84	+7.24			+6.75
$^{206}Pb/^{204}Pb$	18.832	18.855		18.727	18.761			
$^{207}Pb/^{204}Pb$	15.620	15.614		15.582	15.594			
$^{208}Pb/^{204}Pb$	38.742	38.754		38.585	38.642			

The values of Sr, Nd and Pb isotope ratios are quoted with 2σ errors. Mg# is defined as 100 Mg/(Mg + Fe^{2+}) (atomic). The weight ratio Fe_2O_3/FeO is normalized to 0.15. Loss on ignition (LOI) was measured on aliquots of rock powder ignited at 1000°C for one hour. See the text for other details of the analytical methods. Samples: C/1, C/2 and C/3: K-rich basalts; C/4, C/5, C/6 and C/7: basaltic andesites; C/8: dacite.

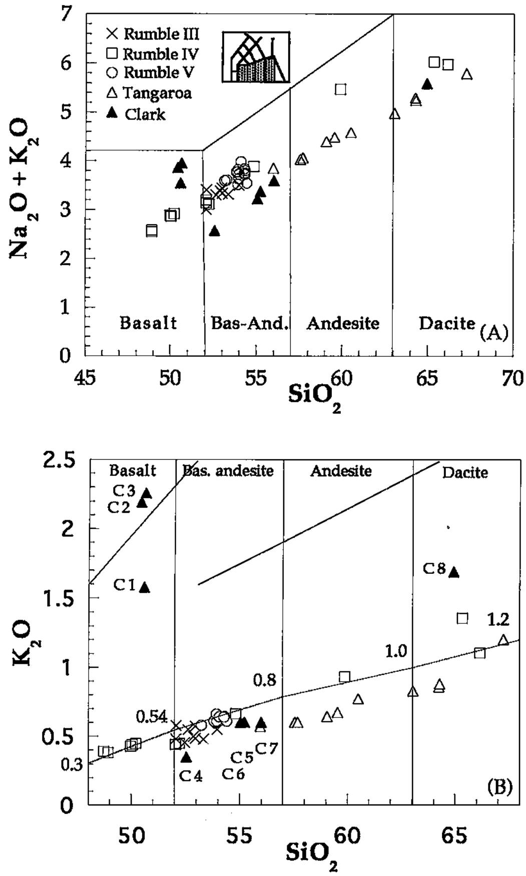

FIG. 5. A. Total alkali ($Na_2O + K_2O$) *versus* SiO_2 (TAS) diagram, with fields from Le Bas *et al.* (1986); B. K_2O *versus* SiO_2 diagrams (from Basaltic Volcanism Study Project (1981). The samples from Clark Volcano are compared to other data from Rumble III, IV and V and Tangaroa volcanoes in the southern Kermadec Arc. All oxides are expressed in weight %.

typically high Ba/La values (*e.g.*, Hawkesworth *et al.* 1993). Relevant to this argument, Gamble *et al.* (1993a) observed a lack of correlation in basalts from TVZ and KA in plots of high field-strength elements (*HFSE*) *versus LILE*, as distinct from plots of selected *HFSE versus HFSE*, which are strongly correlated. Moreover, this decoupling is more apparent for TVZ basalts than for KA basalts, leading to the suggestion that a shortening of across-arc length scales in TVZ source-regions, combined with the relatively recent (<2 Ma) age of volcanism in TVZ, led to heterogeneity in *LILE* abundances in the source.

In Figure 9, we attempt to decipher further the signals of fluid and sediment by plotting ratios of Ba/La *versus* Cs/Sc and Zr/Yb. The rationale behind the use of these ratios is that a high Ba/La ratio should signal "fluid", whereas "sediment", largely owing to its high *LREE* content, will show moderate Ba/La. Elements such as Zr and Yb have a very low potential to partition into a hydrous fluid. Continent-derived sediments should show relatively high Zr/Yb, owing to the presence of detrital zircon. Cs, on the other hand, is demonstrably enriched in sediments, and Sc is relatively impoverished, leading to very high Cs/Sc ratios in sediments. Sources of MORB or depleted MORB (PM in Fig. 9) will have low to very low values of Ba/La, Zr/Yb and Cs/Sc. The observed distribution for basalts from TVZ, KA and the backarc region (Ngatoro Basin and Havre

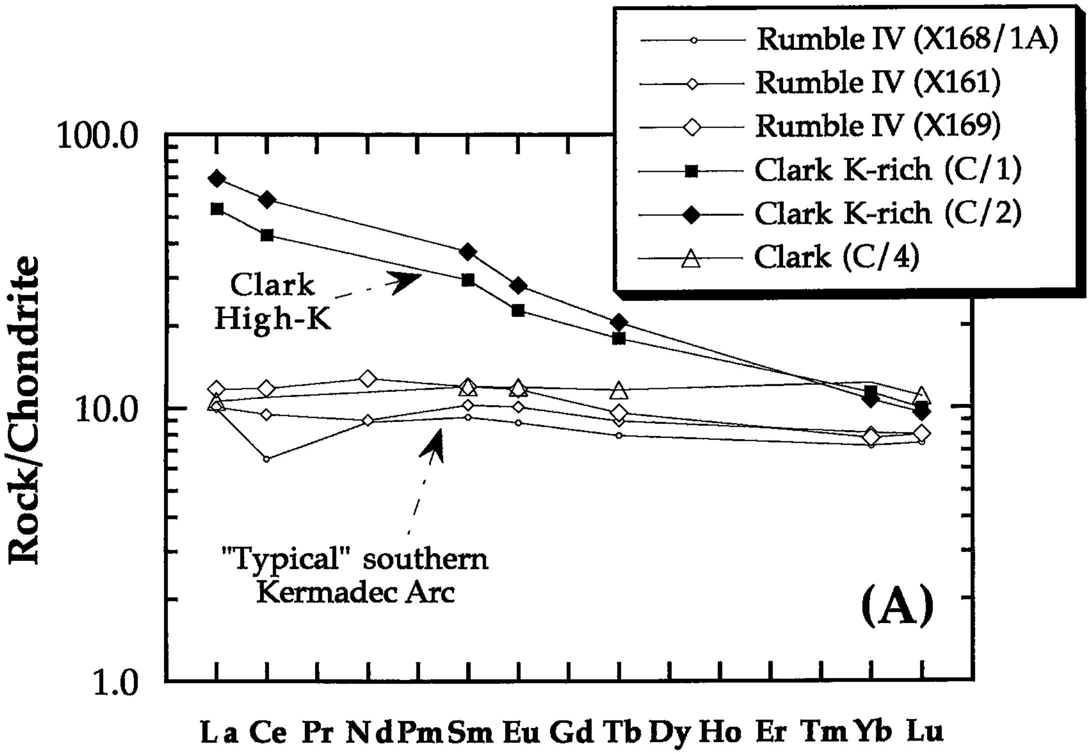

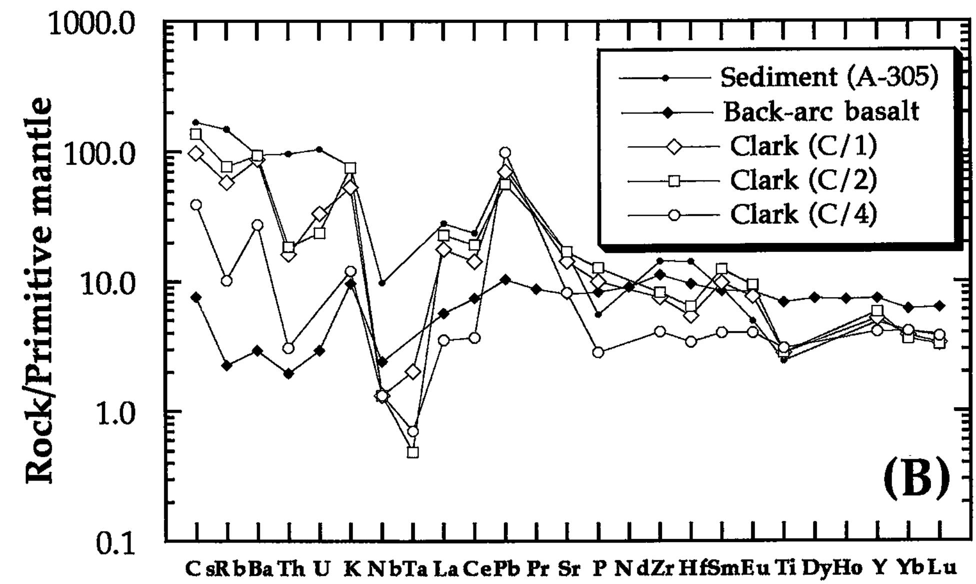

FIG. 6. A. Chondrite-normalized (Wasson & Kellemeyn 1988), concentrations of the rare-earth elements for "typical" southern Kermadec Arc basalts and K-rich basalts (C/1 and C/2) from Clark volcano. B. Primitive mantle-normalized (Sun & Mc Donough 1989) multi-element diagram for K-rich basalts (C/1 and C2) and "typical" Kermadec Arc basalt (C/4) from Clark volcano. Note the *LILE* and *LREE*-enriched nature of the K-rich samples relative to the "typical" KA basalt. A sample of sediment (A–305) from the Hikurangi Trough is shown for comparison, as is a typical basalt from a backarc basin (PPTUW/5 from Havre Trough), both from Gamble *et al.* (1996).

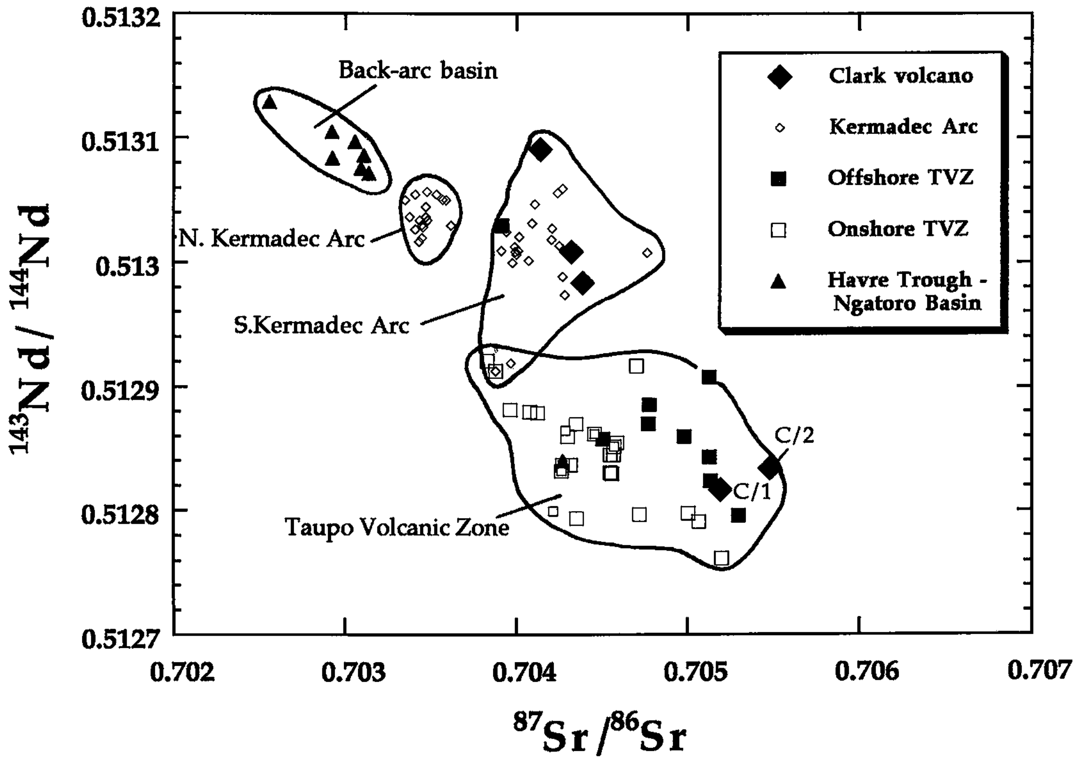

FIG. 7. Plot of $^{87}Sr/^{86}Sr$ *versus* $^{143}Nd/^{144}Nd$ for rocks from Clark Volcano, compared to other rocks from the Kermadec Arc, Havre Trough – Ngatoro Basin and TVZ. The data are taken from Gamble *et al.* (1996).

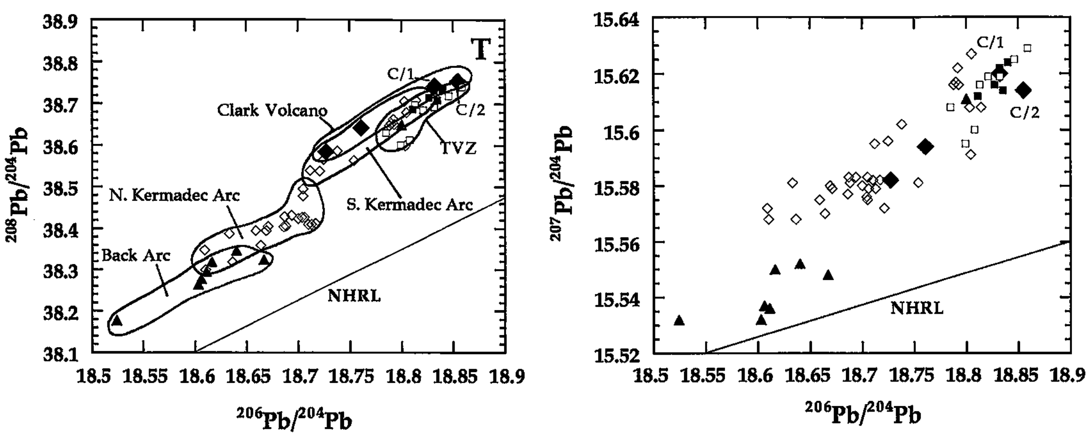

FIG. 8. Pb-isotope plots for rocks from Clark Volcano, compared to rocks from the northern and southern sectors of the Kermadec Arc, TVZ and Havre Trough – Ngatoro Basin. The data are taken from Gamble *et al.* (1996). Symbols as follows: open diamonds: Kermadec Arc, closed diamonds: Clark Volcano, triangles: Havre Trough – Ngatoro Basin backarc basin, open and closed squares: on-shore and off-shore TVZ. The samples of Clark K-rich basalts, C/1 and C/2, are indicated. Note how they overlap with the field of *continental* TVZ rocks. T is average Torlesse metasediment. NHRL is the Northern Hemisphere Reference Line of Zindler & Hart (1986).

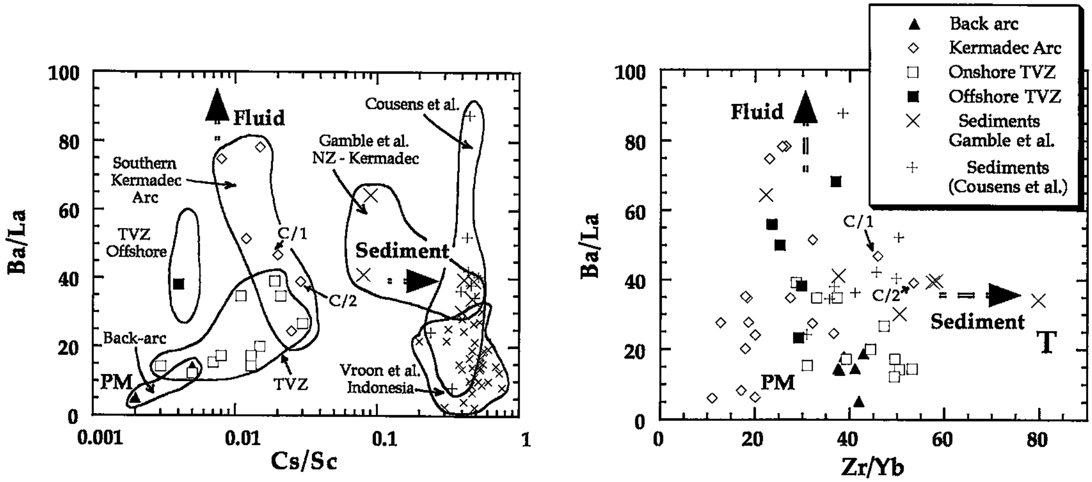

FIG. 9. Plots of Ba/La *versus* Cs/Sc and Zr/Yb for samples of basalt and basaltic andesite from the Kermadec Arc and TVZ. Data on sediments are taken from Gamble *et al.* (1996), Cousens *et al.* (1994), and Vroon *et al.* (1995). PM is primitive mantle (Sun & McDonough 1989). T is average Torlesse metasedimentary basement. The arrows marked "Fluid" and "Sediment" delineate ideal trajectories caused, respectively, by fluid- and sediment-dominated processes. Note the log scale for Cs/Sc.

Trough data, Gamble *et al.* 1994, 1996), fanning out from the origin, is suggestive of variable roles for "fluid" and "sediment", with the northern KA magmas more fluid-dominated, and the southern KA and TVZ magmas sediment-dominated. However, it is interesting to note that no strikingly coherent array of data emerges; as noted previously by Pearce & Peate (1995), this situation may well reflect the complex interplay between fluid and sediment transfer across the slab – mantle interface, together with the tapping of melts from various levels of an integrating melt column.

This model is reasonable geologically, and is also robust with respect to the observed Sr, Nd and Pb isotope data. It may answer the problem of why the Sr-isotope ratios of arc-front basalts from the onshore segment of TVZ are strongly decoupled from the Nd isotope ratios, whereas those from the offshore segment are not (Gamble *et al.* 1994, *cf.* Ellam & Hawkesworth 1988).

K-rich basalts and magma sources

The high K content of the Clark basalts is matched by similarly high concentrations of Rb, Cs, Ba, Sr, elevated abundances of the *LREE* [$5 < (Ce/Yb)_n < 7$] and enriched radiogenic isotopes of Sr, Nd and Pb. Accordingly, they show distinctly elevated values of *LILE/HFSE* and *LILE/REE* such as Ba/La, Cs/La, Ba/Nb, and importantly, a negative Eu-anomaly. In addition, in terms of Mg-number, Ni and Cr contents (being sensitive indicators of crystal fractionation), these K-rich rocks are amongst the most primitive recovered from the southern KA. Nevertheless, these values are low, when compared to those of primary melts equilibrating with mantle peridotite; we conclude that even these melts must have experienced some modification by crystal fractionation.

We therefore need to erect a model whereby primitive magmas with enriched characteristics can be generated in the same mantle column as more "typical" arc magmas. Given these constraints, we list the following possible explanations:

(1) Geochemical characteristics were inherited from a mantle source that is chemically and isotopically distinct from the typical KA source.

(2) Geochemical characteristics were inherited by crustal contamination or some process of assimilation, involving an enriched lithospheric component combined with fractional crystallization (AFC).

(3) Geochemical characteristics were inherited from an isolated source in the sub-arc lithosphere, or some ancient subduction-modified mantle component.

(4) Geochemical characteristics are an extreme example of slab – fluid – sediment interaction.

Of these, we believe that we may rule out 2 and 3, owing to the location of Clark Volcano in an *oceanic* setting and the absence of any pre-Phanerozoic lithosphere in northern New Zealand. Models 1 and 4, however, are not mutually exclusive and, indeed, will be a necessary consequence of slab – mantle-wedge interaction by bulk-sediment mixing, fluid fluxing, or melt transfer, or by some combination of these processes. These form the basis of our petrogenetic model outlined in the following section.

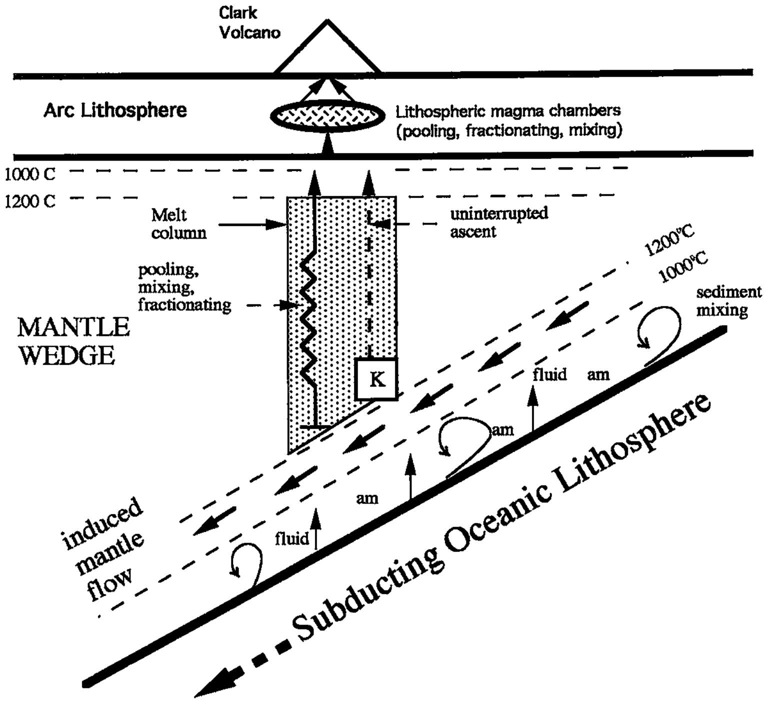

FIG. 10. Model for melt production in the K-rich and "typical" KA suites from Clark Volcano, southern Kermadec Arc (not to scale). Sediment mixing and fluid transfer across the slab – mantle-wedge interface ensures stabilization of amphibole (am) in the wedge of peridotitic mantle. Breakdown of amphibole, enhanced by the induced flow-regime in the wedge and the inverted isotherms (*e.g.*, Davies & Stevenson 1992), results in further transfer of fluid in the mantle wedge. Melts forming and accumulating in the melt column will experience a series of histories varying from limited (the K-rich melts) to extensive pooling and mixing (the "typical" KA melts), at high pressures (in the mantle melt column) and low pressures (in the sub-arc lithosphere). In this model, we envisage the K-rich melts ascending rapidly from a source adjacent to the slab–wedge interface. Depth from volcanic front volcano to slab surface is 112 ± 19 km (Tatsumi 1986).

Preferred petrogenetic hypothesis

There is abundant seismic and bathymetric evidence to show that the Hikurangi Trough has been well supplied by sediment derived from continental New Zealand, and that this sediment-rich portion, together with the Hikurangi Plateau, extends to the southern Kermadec Trench off the southern KA (Lewis 1994, Carter & McCave 1994, Carter *et al.* 1996, Wood & Davy 1994). In contrast, the northern Kermadec Trench has been relatively starved of sediment, and is presently subducting oceanic crust of standard (~7 km) thickness. Gamble *et al.* (1994, 1996) have demonstrated distinctive geochemical differences in basalts from the northern KA toward New Zealand. These differences are manifested by changes in Pb isotopes and element ratios, such as Ba/La and Ce/Yb. Significantly, whereas the TVZ basalts show elevated isotope ratios, and generally higher trace-element ratios such as Ba/La and Ce/Yb relative to the northern KA, they overlap with basalts from the southern KA, despite the fact that one setting is *continental* (TVZ) and the other is *oceanic* (KA). This observation led Gamble *et al.* (1996) to conclude that variable input of sediment, as distinct from crustal contamination, may be the crucial process along the Kermadec – Hikurangi margin.

Furthermore, as indicated by a number of investigators (*e.g.*, Hawkesworth *et al.* 1991, Pearce & Peate 1995), trace elements and isotopes may become decoupled, in the presence of putative hydrous fluids and sediments. In the case of the K-rich basalts from Clark volcano, these basalts extend to higher values of Ba/La and Ce/Yb than most sediments, yet have high Cs/Sc and radiogenic isotopes commensurate with a variable fluid – sediment flux into their source.

Our model (Fig. 10), in part adapted from Tatsumi (1989) and Pearce & Peate (1995), shows a regime in which the K-rich magmas are restricted-volume melts, generated in the lower portion of the melt column adjacent to the slab–mantle interface, which ascend rapidly to the surface, thereby preserving their near-primary status. In this way, their source has been both fluxed by fluid *and* contaminated by subducted sediment, leading to a decoupling of trace elements and isotopes. "Typical" KA melts have experienced pooling higher in the melt column, and thus subsequent mixing and fractionation processes, as they traverse the lithosphere and pond in magma chambers beneath the volcanoes. As a result, phenocrysts in these lavas show manifest textural evidence for disequilibrium and resorption. This type of model provides a satisfactory explanation for the temporally and geographically distinct eruptions of basalt in the region where basalts do not show unambiguous evidence for common parentage or common low-pressure crystal-fractionation pathways (Gamble *et al.* 1990, 1993a). This mechanism also allows for batches of melt to display unusual characteristics, (*e.g.*, TVZ basalts that plot in the KA field and *vice versa*) in that they are chance extracts from a column of accumulating melt.

Conclusions

1) K-rich basalts from Clark volcano at the southern end of the Kermadec Arc offer a rare example of melts formed from a source fluxed by fluids and enriched by subducted sediments.

2) The fact that these basalts coexist with more "typical" Kermadec Arc basalts, and in the volcanic-front tectonic setting, testifies to the complexity of melt-extraction processes from the melt column in the mantle wedge.

3) On the basis of the occurrence described in this paper, the long established "K – depth" relationship should be approached with caution. Melts forming, ascending and accumulating in a dynamic melt-column may show a variety of characteristics determined largely by their point of extraction and the efficiency of ascent.

Furthermore, there is an urgent need for experimental verification of the partitioning and relative diffusivities of *LILE* and *HFSE* among fluid, melt, sediment and peridotitic mantle (*cf.* Pearce & Peate 1995).

Acknowledgements

We thank the officers and crews of the research vessels *Rapuhia, Charles Darwin* and *Akademik Lavrenteyev* for assistance through a number of research cruises. Ken Palmer and Jon Woodhead helped with analytical work at VUW and ANU, respectively. Thanks to Phil Kyle (New Mexico Tech) for the Neutron Activation Analyses. Discussions with Ian Smith, Richard Price, Jon Davidson, Jon Woodhead, Steve Eggins, Chris Hawkesworth and Phil Kyle have been valuable in developing our ideas on subduction-zone magmatism. We thank Graham Nixon and Dana Johnson for organizing an excellent session at GAC/MAC, and Bob Martin, Richard Conrey, Graham Nixon and an anonymous reviewer for their constructive reviews. This work was supported in part by grants from VUW and the Foundation for Research Science and Technology, 93–VIC–8308 (JAG) and 93–WAR–32–384 (ICW).

References

ARMSTRONG, R.L. (1971): Isotopic and chemical constraints on models of magma genesis in volcanic arcs. *Earth Planet. Sci. Lett.* **12**, 137-142.

BASALTIC VOLCANISM STUDY PROJECT (1981): *Basaltic Volcanism on the Terrestrial Planets.* Pergamon Press Inc., New York, N.Y.

BEN OTHMAN, D., WHITE, W.M. & PATCHETT, J. (1989): The geochemistry of marine sediments, island arc magma genesis and crust–mantle recycling. *Earth Planet. Sci. Lett.* **94**, 1-21.

CARTER, L., CARTER, R.M., MCCAVE, I.N. & GAMBLE, J.A. (1996): Regional sediment recycling in the abyssal southwest Pacific Ocean. *Geology* **24**, 735-738.

________ & MCCAVE, I.N. (1994): Development of sediment drifts approaching an active plate margin under the SW Pacific Deep Western Boundary Current. *Paleoceanography* **9**, 1061-1085.

COUSENS, B.L., ALLAN, J.F. & GORTON, M.P. (1994): Subduction-modified pelagic sediments as the enriched component in back-arc basalts from the Japan Sea: Ocean Drilling Program Sites 797 and 794. *Contrib. Mineral. Petrol.* **117**, 421-434.

CRAWFORD, A.J., FALLOON, T.J. & EGGINS, S. (1987): The origin of island arc high-alumina basalts. *Contrib. Mineral. Petrol.* **97**, 417-430.

DAVIES, J.H. & STEVENSON, D.J. (1992): Physical model of source region of subduction zone volcanics. *J. Geophys. Res.* **97**, 2037-2070.

DAVY, B. & WOOD, R. (1994): Gravity and magnetic modelling of the Hikurangi Plateau. *Marine Geol.* **118**, 139-151.

EDWARDS, C.M., MENZIES, M.A. & THIRLWALL, M.F. (1991): Evidence from Muriah, Indonesia, for the interplay of supra-subduction zone and intraplate processes in the genesis of potassic alkaline magmas. *J. Petrol.* **32**, 555-592.

ELLAM, R.M. & HAWKESWORTH, C.J. (1988): Elemental and isotopic variations in subduction related basalts: evidence for a three component model. *Contrib. Mineral. Petrol.* **98**, 72-80.

EWART, A., BROTHERS, R.N. & MATEEN, A. (1977): An outline of the geology and geochemistry, and the possible petrogenetic evolution of the volcanic rocks of the Tonga – Kermadec – New Zealand Island Arc. *J. Volcanol. Geotherm. Res.* **2**, 205-250.

________ & HAWKESWORTH, C.J. (1987): The Pleistocene – Recent Tonga – Kermadec arc lavas: interpretation of new isotopic and rare earth data in terms of a depleted source model. *J. Petrol.* **28**, 495-530.

GAMBLE, J.A., SMITH, I.E.M., GRAHAM, I.J., KOKELAAR, B.P., COLE, J.W., HOUGHTON, B.F. & WILSON, C.J.N. (1990): The petrology, phase relations and tectonic setting of basalts from the Taupo Volcanic Zone, New Zealand, and the Kermadec Island arc – Havre Trough, S.W. Pacific. *J. Volcanol. Geotherm. Res.* **43**, 253-270.

________, ________, MCCULLOCH, M.T., GRAHAM, I.J. & KOKELAAR, B.P. (1993a): The geochemistry and petrogenesis of basalts from the Taupo Volcanic Zone and Kermadec Island Arc, S.W. Pacific. *J. Volcanol. Geotherm. Res.* **54**, 265-290.

________, WOODHEAD, J., WRIGHT, I. & SMITH, I. (1996): Basalt and sediment geochemistry and magma petrogenesis in a transect from oceanic island arc to rifted continental margin arc: the Kermadec –Hikurangi margin, SW Pacific. *J. Petrol.* **37**, 1523-1546.

________ & WRIGHT, I.C. (1995): The Southern Havre Trough: geological structure and magma petrogenesis of an active backarc rift complex. *In* Backarc Basins: Tectonics and Magmatism (B. Taylor, ed.). Plenum Press, New York, N.Y. (29-62).

________, ________ & BAKER, J.A. (1993b): Seafloor geology and petrology in the oceanic to continental transition zone of the Kermadec – Havre – Taupo Volcanic arc system, New Zealand. *N.Z. J. Geol. Geophys.* **36**, 417-435.

________, ________, WOODHEAD, J.D. & MCCULLOCH, M.T. (1994): Arc and back-arc geochemistry in the southern Kermadec arc – Ngatoro Basin and offshore Taupo Volcanic Zone. *In* Volcanism Associated with Extension at Consuming Plate Margins (J.L. Smellie, ed.). *Geol. Soc., Spec. Publ.* **81**, 193-212.

HATHERTON, T. & DICKINSON, W.R. (1969): The relationship between andesitic volcanism and seismicity in Indonesia, the Lesser Antilles, and other island arcs. *J. Geophys. Res.* **74**, 5301-5310.

HAWKESWORTH, C.J., GALLAGHER, K., HERGT, J.M. & MCDERMOTT, F. (1991): Trace element fractionation processes in the generation of island arc basalts. *Phil Trans., R. Soc. London* **A 342**, 179-191.

________, ________, ________ & ________ (1993): Mantle and slab contributions in arc magmas. *Annu. Rev. Earth Planet. Sci.* **21**, 175- 204.

HAWKINS, J., PARSON, L.M., ALLAN, J., *et al.* (1994): Proc. Ocean Drilling Program, Scientific Reports **135**. College Station, Texas.

KARIG, D.E. (1970): Ridges and basins of the Tonga – Kermadec island arc system. *J. Geophys. Res.* **75**, 239-254.

________ (1971): Origin and development of marginal basins in the western Pacific. *J. Geophys. Res.* **76**, 2542-2561.

KUNO, H. (1966): Lateral variation of basalt magma type across continental margins and island arcs. *Bull. Volcanol.* **29**, 195-222.

LE BAS, M.J., LE MAITRE, R.W., STRECKEISEN, A. & ZANETTIN, B. (1986): A chemical classification of igneous rocks based on the total alkali – silica diagram. *J. Petrol.* **27**, 745-750.

LEWIS, K.G. (1994): The 1500-km-long Hikurangi Channel: trench-axis channel that escapes its trench, crosses a plateau, and feeds a fan drift. *Geo-Marine Lett.* **14**, 14-19.

MARSH, B.D. & CARMICHAEL, I.S.E. (1974): Benioff Zone magmatism. *J. Geophys. Res.* **79**, 1196-1206.

MCCULLOCH, M.T. & GAMBLE, J.A. (1991): Geochemical and geodynamical constraints on subduction zone magmatism. *Earth Planet. Sci. Lett.* **102**, 358-374.

MORIMOTO, N., FABRIÈS, J., FERGUSON, A.K., GINSBURG, I.V., ROSS, M., SIEFERT, F.A., ZUSSMAN, J., AOKI, K. & GOTTARDI, G. (1988): Nomenclature of pyroxenes. *Am. Mineral.* **73**, 1123-1133.

MORTIMER, N. & PARKINSON, D. (1996): Hikurangi Plateau: a Cretaceous large igneous province in the southwest Pacific Ocean. *J. Geophys. Res.* **101**, 687-696.

PALMER, K. (1990): XRF analyses of granitoids and associated rocks from South Victoria Land, Antarctica. *Victoria University of Wellington, Research School of Earth Sciences, Geology Board of Studies, Publ.* **5**.

PEARCE, J.A. & PARKINSON, I.J. (1993): Trace element models mantle melting: application to volcanic arc petrogenesis. *In* Magmatic Processes and Plate Tectonics (H.M. Prichard, T. Alabaster, N.B.W. Harris & C.R. Neary, eds.). *Geol. Soc., Spec. Publ.* **76**, 373-403.

________ & PEATE, D.W. (1995): Tectonic implications of the composition of arc magmas. *Annu. Rev. Earth Planet. Sci.* **23**, 251- 285.

PLANK, T. & LANGMUIR, C.H. (1988): An evaluation of global variation in the major element chemistry of arc basalts. *Earth Planet. Sci. Lett.* **90**, 349-370.

________ & ________ (1993): Tracing trace elements from sediment input to volcanic output at subduction zones. *Nature* **362**, 739-743.

SMITH, I.E.M. & BROTHERS, R.N. (1988): Petrology of Rumble seamounts, southern Kermadec Ridge, South West Pacific. *Bull. Volcanol.* **50**, 139-147.

SUN, SHEN-SU & MCDONOUGH, W.F. (1989): Chemical and isotopic systematics of oceanic basalts: implications for mantle composition and processes. *In* Magmatism in the

Oceanic Basins (A.D. Saunders & M.J. Norry, eds.). *Geol. Soc., Spec. Publ.* **42**, 313-345.

TATSUMI, Y. (1986): Formation of the volcanic front in subduction zones. *Geophys. Res. Lett.* **13**, 717-720.

________ (1989): Migration of fluid phases and genesis of basalt magmas in subduction zones. *J. Geophys. Res.* **94**, 4697-4707.

VROON, P.Z., VAN BERGEN, M.J., KLAVER, G.J. & WHITE, W.M. (1995): Strontium, neodymium, and lead isotopic and trace element signatures of the East Indonesian sediments: provenance and implications for Banda Arc magma genesis. *Geochim. Cosmochim. Acta* **59**, 2573-2598.

________, ________, WHITE, W.M. & VAREKAMP, J.C. (1993): Sr–Nd–Pb isotope systematics of the Banda Arc, Indonesia: combined subduction and assimilation of continental material. *J. Geophys. Res.* **98**, 22349-22366.

WASSON, J.T. & KALLEMEYN, G.W. (1988): Compositions of chondrites. *Phil. Trans., R. Soc. Lond.* **A 325**, 535-544.

WOOD, R. & DAVY, B. 1994): The Hikurangi Plateau. *Marine Geol.* **118**, 153-173.

WOODHEAD, J.D., EGGINS, S. & GAMBLE, J.A. (1993): High field strength and transition element systematics in island arc and back-arc basin basalts: evidence for multi-phase melt extraction and a depleted mantle wedge. *Earth Planet. Sci. Lett.* **114**, 491-504.

________, VOLKER, F. & MCCULLOCH, M.T. (1995): Routine Pb isotope determinations using a ^{207}Pb – ^{204}Pb double spike: a long-term assessment of analytical precision and accuracy. *The Analyst* **120**, 35-39.

WRIGHT, I.C. (1992): Shallow structure and active tectonism of an offshore continental back-arc spreading system: the Taupo Volcanic Zone, New Zealand. *Marine Geol.* **103**, 287-309.

________ (1994): Nature and tectonic setting of the southern Kermadec arc volcanoes: an overview. *Marine Geol.* **118**, 217-236.

________, PARSON, L.M. & GAMBLE, J.A. (1996): Evolution and interaction of migrating cross-arc volcanism and back-arc rifting: an example from the southern Havre Trough (35°20' – 37°S). *J. Geophys. Res.* **101**, 22071-22086.

ZINDLER, A. & HART, S.R. (1986): Chemical geodynamics. *Annu. Rev. Earth Planet. Sci.* **14**, 493-571.

Received February 13, 1996, revised manuscript accepted January 5, 1997.